AAC Journals.ASM.org

Azole Affinity of Sterol 14α-Demethylase (CYP51) Enzymes from *Candida albicans* and *Homo sapiens*

Andrew G. Warrilow, Josie E. Parker, Diane E. Kelly, Steven L. Kelly

Institute of Life Science, College of Medicine, Swansea University, Swansea, Wales, United Kingdom

Candida albicans **CYP51 (CaCYP51) (Erg11), full-length** ***Homo sapiens*** **CYP51 (HsCYP51), and truncated Δ60HsCYP51 were expressed in** ***Escherichia coli*** **and purified to homogeneity. CaCYP51 and both HsCYP51 enzymes bound lanosterol (K_s, 14 to 18 μM) and catalyzed the 14α-demethylation of lanosterol using** ***Homo sapiens*** **cytochrome P450 reductase and NADPH as redox partners. Both HsCYP51 enzymes bound clotrimazole, itraconazole, and ketoconazole tightly (dissociation constants [K_ds], 42 to 131 nM) but bound fluconazole (K_d, ~30,500 nM) and voriconazole (K_d, ~2,300 nM) weakly, whereas CaCYP51 bound all five medical azole drugs tightly (K_ds, 10 to 56 nM). Selectivity for CaCYP51 over HsCYP51 ranged from 2-fold (clotrimazole) to 540-fold (fluconazole) among the medical azoles. In contrast, selectivity for CaCYP51 over Δ60HsCYP51 with agricultural azoles ranged from 3-fold (tebuconazole) to 9-fold (propiconazole). Prothioconazole bound extremely weakly to CaCYP51 and Δ60HsCYP51, producing atypical type I UV-visible difference spectra (K_ds, 6,100 and 910 nM, respectively), indicating that binding was not accomplished through direct coordination with the heme ferric ion. Prothioconazole-desthio (the intracellular derivative of prothioconazole) bound tightly to both CaCYP51 and Δ60HsCYP51 (K_d, ~40 nM). These differences in binding affinities were reflected in the observed 50% inhibitory concentration (IC_{50}) values, which were 9- to 2,000-fold higher for Δ60HsCYP51 than for CaCYP51, with the exception of tebuconazole, which strongly inhibited both CYP51 enzymes. In contrast, prothioconazole weakly inhibited CaCYP51 (IC_{50}, ~150 μM) and did not significantly inhibit Δ60HsCYP51.**

Sterol 14α-demethylase (CYP51) is an ancestral activity of the cytochrome P450 superfamily and is required for ergosterol biosynthesis in fungi and cholesterol biosynthesis in mammals (1). Fungal CYP51 (Erg11) is the main target for therapeutic azole antifungal drugs and agricultural azole fungicides. This has led to the development of azole inhibitors that are selective for the fungal CYP51 enzyme over the human homolog and are commonly used to treat fungal infections, including those caused by *Candida albicans* and *Aspergillus fumigatus* (2–4). Agricultural azoles, however, were developed primarily for selectivity against the fungal CYP51 over the plant homolog. The mode of action of azole antifungals involves the nucleophilic nitrogen of the azole heterocyclic ring directly coordinating as the sixth ligand of the heme ferric ion and the azole drug side chains interacting with the CYP51 polypeptide structure (5).

Many yeasts and fungi that are causative agents of clinical infections, such as *Candida* species and *Aspergillus* species, are also present in the general environment and are exposed to the selective pressure of agricultural azoles in the field. This has led to concerns that azole-resistant strains of yeasts and fungi responsible for clinical infections are emerging due to the use of agricultural azole fungicides on crops raising azole tolerance/resistance among environmental strains (6). Recently, a point mutation in *A. fumigatus* CYP51A that confers resistance to azole antifungal agents was attributed to resistance acquired outside the clinic, in the general environment (6–8).

The increasing emergence of azole-resistant yeast and fungal strains is due to the prophylactic use of azole drugs, prolonged treatment regimens in the clinic, and, potentially, usage of agricultural azole fungicides in crop protection (9–14). This necessitates the development of new azole antifungal compounds with increased selectivity for the fungal CYP51 enzyme over the human homolog and alternative antifungal strategies and treatment regimens against drug-resistant strains. Currently, new azole and nonazole CYP51 inhibitors are being developed for the next generation of antifungal drugs (15–22).

Besides concerns over the influence of agricultural azoles on resistance development in the clinic, concern has arisen in Europe over endocrine disruption effects of agricultural azoles in mammals (23, 24) and the hepatotoxicity of these fungicides (25). Azole antifungals cause hepatotoxicity by inducing the expression of liver cytochrome P450 enzymes (CYP1, CYP2, and CYP3 families), which in turn increases the abundance of reactive oxygen species in liver cells, resulting in lipid peroxidation and DNA damage (25). In addition, azole antifungals have the potential to inhibit liver P450 enzymes, interfering in the phase I metabolism of xenobiotics (25–28). Ketoconazole and itraconazole, but not fluconazole, induced CYP1A1 expression in mice (25), and propiconazole induced CYP2B10, CYP3A11, CYP2C55, and CYP2C65 expression in mice (26), along with the formation of benign and malignant liver tumors. Disruption of the endocrine system can lead to impaired reproduction, alterations in sexual differentiation, impaired growth and development, and the formation of hormone-dependent cancers (24). Ketoconazole causes the demasculinizing of male fetuses in rats (23) and decreased levels of testosterone and cortisol in the plasma of humans (29, 30), leading to gynecomastia and oligospermia in men and menstrual irregularities in women (31). Azole antifungals disrupt the endocrine system by inhibiting several highly substrate-selective cytochrome

Received 9 October 2012 **Returned for modification** 10 December 2012
Accepted 24 December 2012
Published ahead of print 28 December 2012
Address correspondence to Steven L. Kelly, s.l.kelly@swansea.ac.uk.

doi:10.1128/AAC.02067-12

P450 enzymes involved in mammalian steroid hormone biosynthesis (24). These include aromatase (CYP19) (which catalyzes the C-10 demethylation of androgens to estrogens), CYP11A (which converts cholesterol to pregnenolone), steroid 21-hydroxylase (CYP21), aldosterone synthase (CYP11B2), steroid 11β-hydroxylase (CYP11B1), steroid 17α-hydroxylase/17,20-lyase (CYP17), and lanosterol 14α-demethylase (CYP51), disturbing the *in vivo* hormonal balance.

In terms of increased safety, selective compounds that inhibit fungal CYP51 and not human CYP51 are desirable. Comparisons of activity have not included agricultural azoles and pure CYP51 forms but have relied instead on microsomal fractions. In this study, we expressed *C. albicans* CYP51 (CaCYP51) and the full-length form and a solubilized form (Δ60) of *Homo sapiens* CYP51 (HsCYP51) in *Escherichia coli*, purifying all three to homogeneity. We performed detailed azole binding studies using UV-visible spectroscopy under oxidative conditions and using five therapeutic azole antifungal drugs (clotrimazole, fluconazole, itraconazole, ketoconazole, and voriconazole) and seven agricultural azole fungicides (epoxiconazole, prochloraz, propiconazole, prothioconazole, prothioconazole-desthio, tebuconazole, and triadimenol). In addition, 50% inhibitory concentration (IC_{50}) determinations for each azole were made using a CYP51 reconstitution assay system. The potential inhibitory action against CaCYP51 and the undesired side effect of inhibiting HsCYP51 were assessed, and the relative selectivity of each compound for the fungal enzyme was determined. Understanding which structural elements of azole antifungal drugs confer increased selectivity for the fungal CYP51 enzyme over the human homolog will assist in the design of the next generation of azole antifungals for agriculture as well as the clinic.

MATERIALS AND METHODS

Construction of pCWori$^+$-*CaCYP51*, pCWori$^+$-*HsCYP51*, and pCWori$^+$-Δ*60HsCYP51* expression vectors. The pCWori$^+$-*CaCYP51* expression construct containing the *C. albicans CYP51* gene (UniProtKB accession number P10613, *ERG11*) was created as described previously (4). The pCWori$^+$-*HsCYP51* and pCWori$^+$-Δ*60HsCYP51* expression constructs were created by inserting the full-length *H. sapiens CYP51* gene (UniProtKB accession number Q16850) and Δ60 truncated *H. sapiens CYP51* gene (synthesized by GeneCust, Dudelange, Luxembourg) into the pCWori$^+$ vector using NdeI and HindIII cloning sites. The Δ*60HsCYP51* gene truncation replaced the N-terminal transmembrane domain upstream of Pro-61 with the N-terminal MAKKTSSKGKL sequence from CYP2C3 (32, 33). The first eight amino acids of both the *CaCYP51* and *HsCYP51* constructs were altered to MALLLAVF (ATGGCTCTGTTATT AGCAGTTTTT) to facilitate the expression in *E. coli* (34). All three expression constructs included a 12-base insertion (CATCACCATCAC), encoding a four-histidine tag immediately in front of the stop codon, to facilitate protein purification by Ni^{2+}-nitrilotriacetic acid (NTA) agarose affinity chromatography.

Heterologous expression in *E. coli* and isolation of recombinant CaCYP51, HsCYP51, and Δ60HsCYP51 proteins. The three pCWori$^+$-*CYP51* constructs were transformed into competent *E. coli* DH5α cells, and transformants were selected using 0.1 mg ml^{-1} ampicillin. The growth and expression conditions were the same as those reported previously (4) except that the expression temperature for Δ60HsCYP51 was 29°C. Protein isolation was performed according to the method of Arase et al. (35) except that 2% sodium cholate was used in the sonication buffer. The solubilized CYP51 proteins were purified by affinity chromatography using Ni^{2+}-NTA agarose as described previously (36), except that 0.1% L-histidine in 0.1 M Tris-HCl (pH 8.1) and 25% glycerol was used to elute nonspecifically bound *E. coli* proteins after the salt washes. CYP51 proteins were recovered by elution with 1% L-histidine in 0.1 M Tris-HCl (pH 8.1) and 25% glycerol, followed by dialysis against 5 liters of 25 mM Tris-HCl (pH 8.1) and 10% glycerol. Ni^{2+}-NTA-agarose-purified CYP51 proteins were used for all subsequent spectral and IC_{50} determinations. Protein purity was assessed by SDS-polyacrylamide gel electrophoresis with Coomassie brilliant blue R-250 staining.

Determination of cytochrome P450 protein concentrations. Reduced carbon monoxide difference spectra (37) were used to determine P450 concentrations, with carbon monoxide passed through the cytochrome P450 solution prior to the addition of sodium dithionite to the sample cuvette. An extinction coefficient of 91 mM^{-1} cm^{-1} (38) was used to calculate cytochrome P450 concentrations from the absorbance difference between 445 to 447 nm and 490 nm. Absolute spectra were determined between 700 and 300 nm using 5 μM CYP51 in 0.1 M Tris-HCl (pH 8.1) and 25% glycerol as described previously (36). Confirmation that isolated CaCYP51, HsCYP51, and Δ60HsCYP51 proteins were active was obtained by measuring the 14α-demethylation of lanosterol using the CYP51 reconstitution assay detailed below.

CYP51 reconstitution assay system. IC_{50} determinations were performed using the CYP51 reconstitution assay system (final reaction volume, 500 μl) containing 1 μM CaCYP51, 1 μM HsCYP51, or 0.4 μM Δ60HsCYP51, 2 μM *H. sapiens* cytochrome P450 reductase (CPR) (UniProtKB accession number P16435), 60 μM lanosterol, 50 μM dilaurylphosphatidylcholine, 4% (wt/vol) 2-hydroxypropyl-β-cyclodextrin, 0.4 mg ml^{-1} isocitrate dehydrogenase, 25 mM trisodium isocitrate, 50 mM NaCl, 5 mM $MgCl_2$, and 40 mM MOPS (morpholinepropanesulfonic acid) (pH ~7.2), as described previously (19). Azole antifungal agents were added in 2.5 μl dimethylformamide, followed by a 10-min incubation at 37°C prior to assay initiation with 4 mM β-NADPH-Na_4. Samples were then shaken for 10 min (CaCYP51) or 4 min (HsCYP51 and Δ60HsCYP51) at 37°C. Sterol metabolites were recovered by extraction with ethyl acetate followed by derivatization with *N*,*O*-bis(trimethylsilyl)trifluoroacetamide and tetramethylsilane prior to analysis by gas chromatography-mass spectrometry (39). Enzyme velocities were calculated from the gas chromatograms by determining the ratio of product to substrate, calibrated against lanosterol standards, to obtain the nmol of demethylated product in each assay, which, when divided by the nmol of CYP51 in the assay system and the incubation time, gave velocities expressed in min^{-1}. The IC_{50} in this study is defined as the inhibitor concentration causing 50% inhibition of CYP51 activity under the stated assay conditions.

Azole binding studies. Binding of azole antifungal agents to 5 μM CaCYP51, HsCYP51 (medical azoles only), and Δ60HsCYP51 proteins was performed as described previously (2) using quartz cuvettes with a 4.5-mm light path. Stock 1-, 0.5-, 0.2-, and 0.1-mg ml^{-1} solutions of the medical azole antifungals clotrimazole, fluconazole, itraconazole, ketoconazole, and voriconazole and the agricultural azole antifungals epoxiconazole, prochloraz, propiconazole, prothioconazole, prothioconazole-desthio, tebuconazole, and triadimenol were prepared in dimethylformamide. Azole antifungals were progressively titrated against 5 μM CYP51 proteins in 0.1 M Tris-HCl (pH 8.1) and 25% glycerol at 22°C, and equivalent volumes of dimethylformamide were also added to the CYP51-containing compartment of the reference cuvette. The absorbance difference spectra between 500 and 350 nm were determined after each incremental addition of azole, with binding saturation curves constructed as $\Delta A_{peak-trough}$ plotted against azole concentration. The dissociation constant (K_d) of the enzyme-azole complex for each azole was determined by nonlinear regression (Levenberg-Marquardt algorithm) using a rearrangement of the Morrison equation for tight ligand binding (40, 41). Tight binding is normally observed when the K_d for a ligand is similar to or lower than the concentration of the enzyme present (42). When ligand binding was weak, the Michaelis-Menten equation was used to fit the data. Each binding determination was performed in triplicate. The chemical

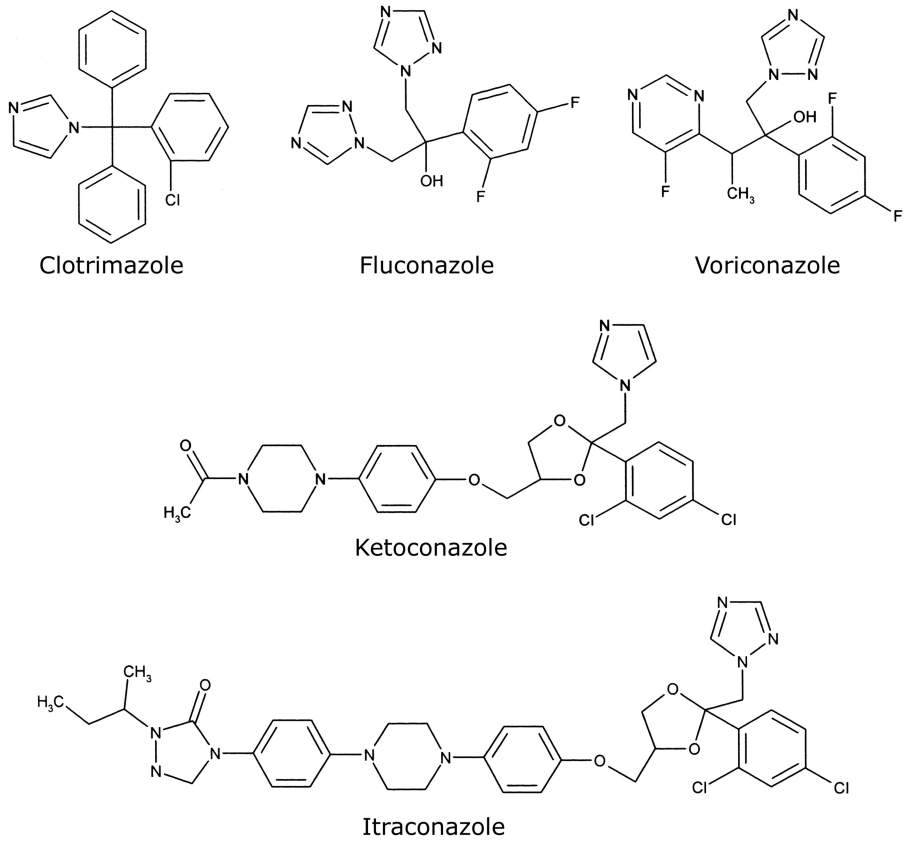

FIG 1 Chemical structures of medical azole antifungal agents. The chemical structures of clotrimazole (molecular weight [MW], 345), fluconazole (MW, 306), voriconazole (MW, 349), ketoconazole (MW, 531), and itraconazole (MW, 706), which were used in this study, are shown.

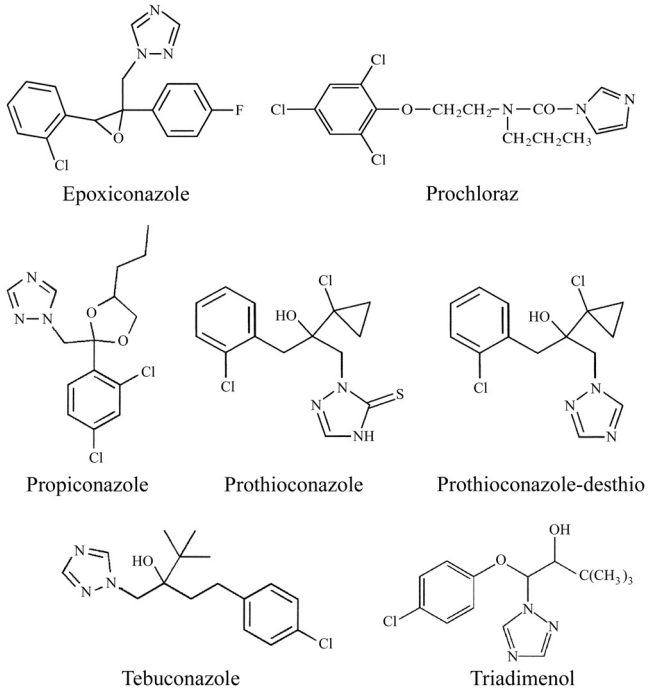

FIG 2 Chemical structures of agricultural azole antifungal agents. The chemical structures of epoxiconazole (molecular weight [MW], 330), prochloraz (MW, 377), propiconazole (MW, 342), prothioconazole (MW, 344), prothioconazole-desthio (MW, 312), tebuconazole (MW, 308), and triadimenol (MW, 296), which were used in this study, are shown.

structures of the azole antifungals used in this study are shown in Fig. 1 and 2.

Data analysis. Curve fitting of the ligand binding data was performed using the computer program ProFit 6.1.12 (QuantumSoft, Zurich, Switzerland). Spectral determinations were made using quartz semi-micro cuvettes with a Hitachi U-3310 UV-visible spectrophotometer (San Jose, CA).

Chemicals. All chemicals, including the azole antifungals except voriconazole, were obtained from the Sigma Chemical Company (Poole, United Kingdom). Voriconazole was supplied by Discovery Fine Chemicals (Bournemouth, United Kingdom). Growth media, sodium ampicillin, isopropyl-β-D-thiogalactopyranoside (IPTG), and 5-aminolevulenic acid were obtained from Foremedium Ltd. (Hunstanton, United Kingdom). The Ni^{2+}-NTA agarose affinity chromatography matrix was obtained from Qiagen (Crawley, United Kingdom).

RESULTS

Expression and purification of CaCYP51, HsCYP51, and Δ60HsCYP51 proteins. Cholate extraction using sonication (35) yielded 270 ± 37, 20 ± 5, and 645 ± 68 (mean ± SD) nmol per liter culture of CaCYP51, HsCYP51, and Δ60HsCYP51, respectively, as determined by carbon monoxide difference spectroscopy (37). Expression levels of CaCYP51 were comparable to those obtained previously (4, 43, 44), as were the levels of expression of Δ60HsCYP51 (44), in contrast to the low expression levels of HsCYP51. Purification by Ni^{2+}-NTA agarose chromatography resulted in 54%, 92%, and 63% recoveries for native CaCYP51, HsCYP51, and Δ60HsCYP51, respectively. SDS-polyacrylamide gel electrophoresis confirmed the purity of the Ni^{2+}-NTA-aga-

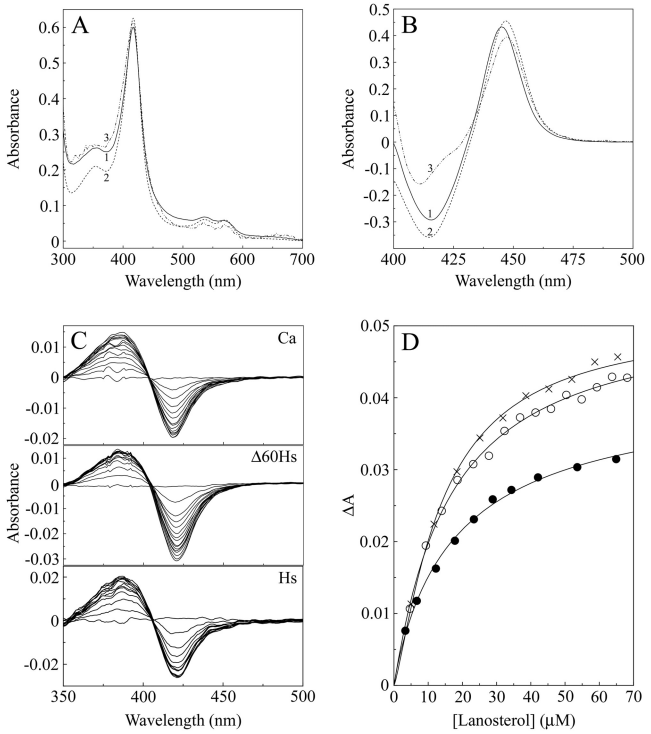

FIG 3 Spectral properties of CaCYP51, Δ60HsCYP51, and HsCYP51. (A and B) Absolute oxidized absorption spectra (A) between 700 and 300 nm and reduced carbon monoxide difference spectra (B) between 500 and 400 nm were determined using 5 μM CaCYP51 (line 1), Δ60HsCYP51 (line 2), and HsCYP51 (line 3), with matched quartz semi-micro cuvettes with 10-mm light paths. (C) Type I difference spectra were obtained by progressive titration of lanosterol against 5 μM solutions of the three CYP51 proteins using quartz semi-micro cuvettes with 4.5-mm light paths. (D) Lanosterol saturation curves were constructed for the CaCYP51 (●), Δ60HsCYP51 (○), and HsCYP51 (×) proteins. All spectral determinations were performed in triplicate, although the results from only one replicate are shown.

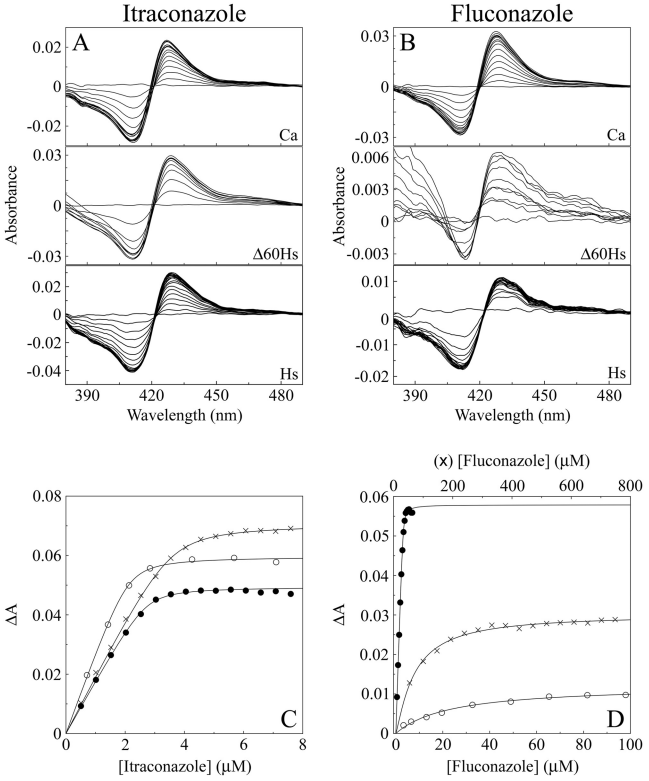

FIG 4 Itraconazole and fluconazole binding with CaCYP51, Δ60HsCYP51, and HsCYP51. (A and B) Type II difference spectra were obtained for 5 μM solutions of the three CYP51 proteins by progressive titration with itraconazole (A) and fluconazole (B). (C and D) Azole saturation curves were constructed for itraconazole (C) and fluconazole (D) as the change in absorbance ($\Delta A_{peak-trough}$) against azole concentration using a rearrangement of the Morrison equation (40) for the tight ligand binding observed with CaCYP51 (●), Δ60HsCYP51 (○), and HsCYP51 (×).

rose-eluted CYP51 proteins to be greater than 95% when assessed by staining intensity, with apparent molecular weights of 61,000 for CaCYP51, 57,000 for HsCYP51, and 53,000 for Δ60HsCYP51, which were close to the predicted values of 61,221, 55,771, and 52,394, respectively, including the four-histidine C-terminal extensions.

Spectral properties of recombinant CYP51 proteins. The absolute spectra of the resting oxidized forms of all three CYP51 proteins (Fig. 3A) were similar. CaCYP51 had α, β, Soret (γ), and δ spectral bands at 565, 536, 417, and 356 nm, respectively, compared to 570, 534, 417, and 353 nm for HsCYP51 and 570, 536, 417, and 354 nm for Δ60HsCYP51. These spectral characteristics were typical of a ferric cytochrome P450 enzyme predominantly (~80%) in the low-spin state (36, 45). Reduced carbon monoxide difference spectra (Fig. 3B) produced the characteristic red-shifted Soret peak at 445 to 447 nm typical of ferrous cytochrome P450 enzymes complexed with CO (37, 38). All three CYP51 proteins bound lanosterol to produce type I binding spectra (Fig. 3C) typical of the interaction of substrates with cytochromes P450 (45), with a peak at 386 nm and a trough at 419 nm. Substrate binding constant (K_s) values for lanosterol of 13.5 ± 1.1, 17.9 ± 1.6, and 18.4 ± 1.5 μM determined from the substrate saturation curves (Fig. 3D) for CaCYP51, HsCYP51, and Δ60HsCYP51, respectively, confirmed that the three CYP51 proteins had affinities for lanosterol that were similar. All three CYP51 proteins were functionally active after isolation, with velocities of 3.9, 6.1, and 22.7 min^{-1} for CaCYP51, HsCYP51, and Δ60HsCYP51, respectively, using *H. sapiens* cytochrome P450 reductase (CPR) and NADPH as redox partners. Interestingly, the turnover number for HsCYP51 was 3.7-fold lower than that for the truncated Δ60 form of the enzyme, suggesting that the N-terminal membrane anchor impedes optimal catalysis in the *in vitro* CYP51 reconstitution assay.

Binding studies with medical azole antifungals. Clotrimazole, itraconazole (Fig. 4A), fluconazole (Fig. 4B), ketoconazole, and voriconazole all bound tightly to CaCYP51, producing type II binding spectra with peaks at 429 to 431 nm and troughs at 411 to 413 nm. Type II binding spectra are caused by the triazole ring N-4 nitrogen (fluconazole, itraconazole, and voriconazole) or the imidazole ring N-3 nitrogen (clotrimazole and ketoconazole) coordinating as the sixth ligand with the heme iron (5) to form the low-spin CYP51-azole complex, resulting in a "red shift" of the heme Soret peak. Both HsCYP51 and Δ60HsCYP51 bound fluconazole weakly and voriconazole less strongly than CaCYP51, while clotrimazole, itraconazole, and ketoconazole bound slightly less strongly to HsCYP51 and Δ60HsCYP51 than CaCYP51 (Table 1). This was reflected in the calculated K_d values; HsCYP51 and

TABLE 1 Binding parameters for medical azoles with CaCYP51, Δ60HsCYP51, and HsCYP51[a]

Medical azole antifungal	CaCYP51		Δ60HsCYP51		HsCYP51		Fold difference in K_d	
	K_d (nM)	ΔA_{max}	K_d (nM)	ΔA_{max}	K_d (nM)	ΔA_{max}	Δ60HsCYP51/ CaCYP51	HsCYP51/ CaCYP51
Clotrimazole	26 ± 6	0.0615 ± 0.0015	55 ± 5	0.0964 ± 0.0028	65 ± 19	0.1091 ± 0.0069	2.1	2.5
Fluconazole	56 ± 4	0.0595 ± 0.0016	30,400 ± 4,100	0.0144 ± 0.0006	30,500 ± 7,700	0.0299 ± 0.0047	543	545
Itraconazole	19 ± 5	0.0493 ± 0.0014	92 ± 7	0.0533 ± 0.0048	131 ± 13	0.0707 ± 0.0036	4.8	6.9
Ketoconazole	12 ± 3	0.1073 ± 0.0019	42 ± 16	0.1315 ± 0.0063	61 ± 17	0.1284 ± 0.0081	3.5	5.1
Voriconazole	10 ± 2	0.0590 ± 0.0032	2,290 ± 120	0.0775 ± 0.0021	2,240 ± 520	0.0480 ± 0.0031	229	224

[a] CYP51 concentrations of 5 μM were used. A rearrangement of the Morrison equation was used to determine K_d values for the ligands with tight binding (40). Mean K_d and ΔA_{max} values of three replicates are shown with the associated standard deviations.

Δ60HsCYP51 had 540-fold-lower affinities for fluconazole and 220-fold-lower affinities for voriconazole, in comparison to just 2.5- to 2.1-fold-lower affinities for clotrimazole, than CaCYP51 (Table 1). Itraconazole and ketoconazole bound tightly to HsCYP51 and Δ60HsCYP51, with only 6.9- to 4.8-fold- and 5.1- to 3.5-fold-lower affinities, respectively, than CaCYP51 (Table 1). With the exception of the catalytic turnover number, HsCYP51 behaved nearly identically to Δ60HsCYP51 in terms of spectral properties and binding of lanosterol and the five medical azole antifungal agents, confirming the validity of the published crystal model for truncated human CYP51 (46). Therefore, the remaining studies were performed using Δ60HsCYP51 alone in comparison with CaCYP51 because of the low yield of HsCYP51 from expression in *E. coli*.

Binding studies with agricultural azole antifungals. Both CaCYP51 and Δ60HsCYP51 bound epoxiconazole (Fig. 5A), propiconazole (Fig. 5B), prochloraz, tebuconazole, and triadimenol tightly. Δ60HsCYP51 had a 5-fold-lower affinity for epoxiconazole, a 9-fold-lower affinity for propiconazole, a 7-fold-lower affinity for prochloraz, a 3-fold-lower affinity for tebuconazole, and a 5-fold-lower affinity for triadimenol than CaCYP51 (Table 2). The selectivity of these five agricultural azole antifungals for the fungal CaCYP51 target enzyme (K_ds, 22 to 68 nM) over the human CYP51 enzyme (K_ds, 115 to 359 nM) was relatively poor at only 3- to 9-fold.

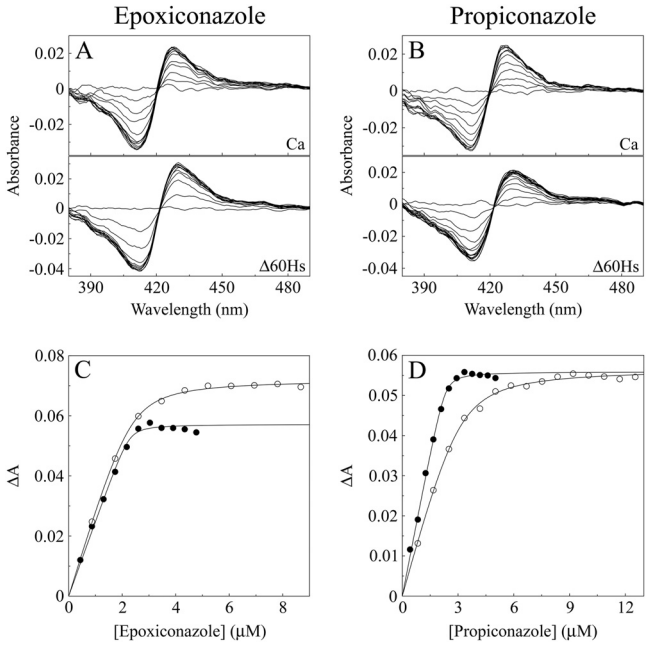

FIG 5 Epoxiconazole and propiconazole binding with CaCYP51 and Δ60HsCYP51. (A and B) Type II difference spectra were obtained for 5 μM CaCYP51 and Δ60HsCYP51 by progressive titration with epoxiconazole (A) and propiconazole (B). (C and D) Azole saturation curves were constructed for epoxiconazole (C) and propiconazole (D) as the change in absorbance ($\Delta A_{peak-trough}$) against azole concentration using a rearrangement of the Morrison equation (40) for the tight ligand binding observed with CaCYP51 (●) and Δ60HsCYP51 (○).

Prothioconazole bound weakly to both CaCYP51 and Δ60HsCYP51, producing type I binding spectra (Fig. 6A). Type I difference spectra are often associated with, but not exclusively caused by, substrate or substrate analog binding and are indicative of a change in the cytochrome P450 spin state from low spin (hexa-coordinated) to high spin (penta-coordinated) with displacement of the hexa-coordinated water molecule from the heme (45). This indicates that prothioconazole does not directly coordinate with the heme ferric ion; therefore, prothioconazole does not behave like a typical azole antifungal agent when binding to CYP51. The weak binding was reflected by high apparent K_d values of 6,100 and 910 nM for prothioconazole with CaCYP51 and Δ60HsCYP51, respectively. However, when the sulfur atom is removed from the triazole ring of prothioconazole to form prothioconazole-desthio (Fig. 2), the desthio form binds tightly to the two CYP51 proteins (Fig. 6B) with similar affinities (K_d, ~40 nM), suggesting that the desthio form of prothioconazole is the active fungicidal agent.

IC_{50} determinations for azole antifungal agents. IC_{50} determinations using 60 μM lanosterol and 1 μM CaCYP51 with the medical azoles fluconazole, itraconazole, and ketoconazole (Fig. 7A) confirmed that all three azoles bound tightly to CaCYP51, causing severe inhibition of CYP51 activity. The IC_{50}s for all three azoles were between 0.4 and 0.6 μM (Table 3), half of the CaCYP51 concentration present, indicating direct tight 1:1 binding between the azole and CaCYP51, with lanosterol being unable to displace these three azoles from CaCYP51. Similar results were obtained for fluconazole with CaCYP51 using truncated Δ33 *Saccharomyces cerevisiae* CPR (4), suggesting that the partner CPR did not affect the observed IC_{50}. With 0.4 μM Δ60HsCYP51 (Fig. 7B), inhibition by fluconazole was poor, with a calculated IC_{50} of ~1,300 μM (Table 3) and only a 25% reduction in CYP51 activity observed in the presence of 653 μM fluconazole, which was in agreement with the high K_d value for fluconazole with Δ60HsCYP51 (Table 1). Ketoconazole strongly inhibited Δ60HsCYP51 activity, with an IC_{50} of 4.5 μM, 11-fold higher than the CYP51 concentration present, indicating that the binding was not as tight as that observed with CaCYP51 and that lanosterol was able to

TABLE 2 Binding parameters for agricultural azoles with CaCYP51 and Δ60HsCYP51[a]

Agricultural azole antifungal	CaCYP51		Δ60HsCYP51		Fold difference in K_d, Δ60HsCYP51/CaCYP51
	K_d (nM)	ΔA_{max}	K_d (nM)	ΔA_{max}	
Epoxiconazole	22 ± 6	0.0571 ± 0.0018	115 ± 9	0.0775 ± 0.0031	5.2
Prochloraz	49 ± 2	0.0714 ± 0.0049	325 ± 51	0.0674 ± 0.0006	6.6
Propiconazole	38 ± 10	0.0575 ± 0.008	335 ± 37	0.0562 ± 0.0042	8.8
Prothioconazole	6,100 ± 960[b]	0.0136 ± 0.0002	910 ± 290[b]	0.0105 ± 0.0014	0.15
Prothioconazole-desthio	41 ± 3	0.0760 ± 0.0031	39 ± 4	0.0824 ± 0.0036	0.95
Tebuconazole	36 ± 3	0.0538 ± 0.0022	118 ± 10	0.0759 ± 0.0044	3.3
Triadimenol	68 ± 4	0.0487 ± 0.0006	359 ± 38	0.0492 ± 0.0015	5.3

[a] CYP51 concentrations of 5 μM were used. A rearrangement of the Morrison equation was used to determine K_d values for the ligands with tight binding (40). Mean K_d and ΔA_{max} values of three replicates are shown with the associated standard deviations.
[b] The Michaelis-Menten equation was used to determine K_d values for prothioconazole.

displace ketoconazole from Δ60HsCYP51. Interestingly, the IC_{50} for itraconazole with Δ60HsCYP51 was greater at 70 μM than suggested by the K_d value of 92 nM (Table 1), indicating that, even though itraconazole binds tightly to Δ60HsCYP51, lanosterol is able to displace itraconazole from Δ60HsCYP51 under the assay conditions. Even in the presence of 283 μM itraconazole, Δ60HsCYP51 retained 32% of the azole-free CYP51 activity.

IC_{50} determinations using 60 μM lanosterol and 1 μM CaCYP51 with the seven agricultural azoles (Fig. 7C) indicated that the observed inhibition was more variable than that observed with the medical azoles (Table 3). Epoxiconazole, propiconazole, prothioconazole-desthio, prochloraz, and tebuconazole strongly inhibited CaCYP51 activity, with IC_{50}s of 0.5, 0.6, 0.6, 0.7, and 0.9 μM, respectively, with epoxiconazole and propiconazole in particular approaching the potency of itraconazole as a severe inhibitor of CaCYP51 activity. The ability of the 60 μM lanosterol present in the assay system to displace these azoles from CaCYP51, as measured by residual activity with 4 μM azole, gradually increased, with residual activity levels of 1% for epoxiconazole, 2.3% for propiconazole, 3.9% for tebuconazole, 6.3% for prothioconazole-desthio, and 9.6% for prochloraz being observed. Triadimenol inhibited CaCYP51 less severely than the other agricultural azoles (except prothioconazole), with an IC_{50} of 1.3 μM and a residual CYP51 activity of 10.2% with 4 μM triadimenol, indicating a significantly lower potency against CaCYP51 than itracona-

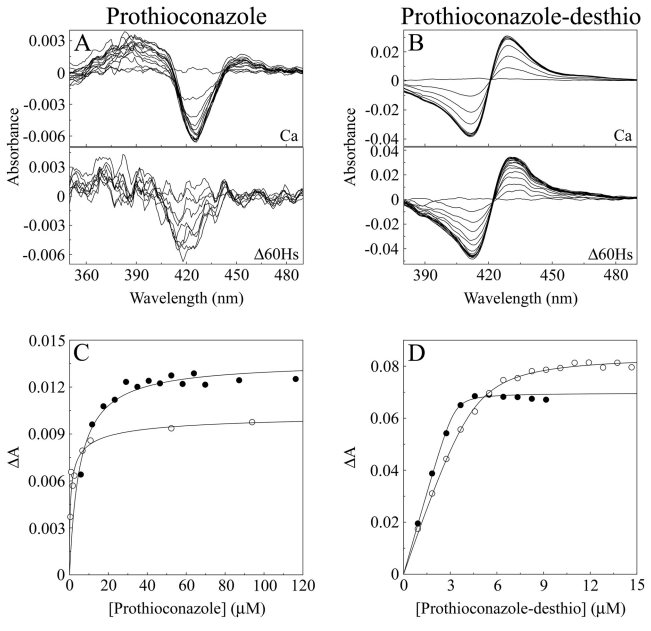

FIG 6 Prothioconazole and prothioconazole-desthio binding with CaCYP51 and Δ60HsCYP51. (A and B) Type II difference spectra were obtained for 5 μM CaCYP51 and Δ60HsCYP51 by progressive titration with prothioconazole (A) and prothioconazole-desthio (B). (C and D) Azole saturation curves were constructed for prothioconazole (C) and prothioconazole-desthio (D) as the change in absorbance ($\Delta A_{peak - trough}$) against azole concentration. Prothioconazole-desthio saturation curves were fitted using a rearrangement of the Morrison equation (40) for the tight ligand binding observed with CaCYP51 (●) and Δ60HsCYP51 (○). The Michaelis-Menten equation was used to fit the weak binding observed with prothioconazole.

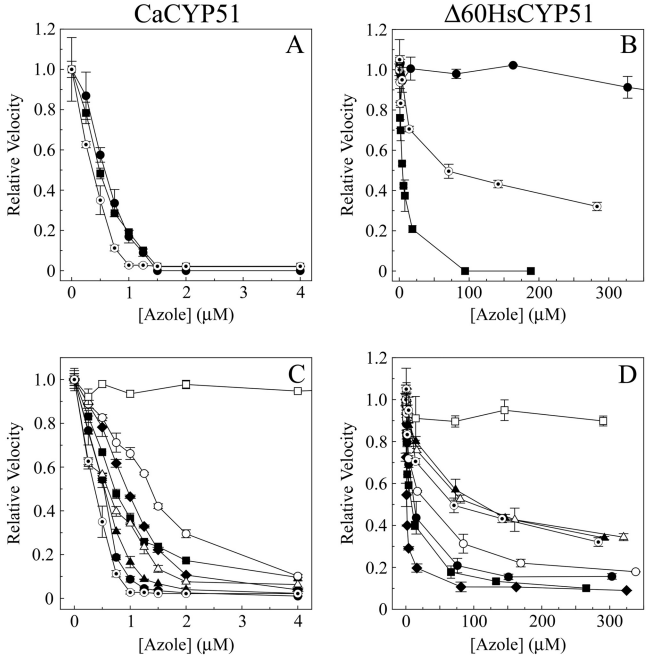

FIG 7 Azole IC_{50} determinations with CaCYP51 and Δ60HsCYP51. (A and B) IC_{50}s were determined with 1 μM CaCYP51 (A) and 0.4 μM Δ60HsCYP51 (B) for the medical azoles fluconazole (●), itraconazole (⊙), and ketoconazole (■). (C and D) IC_{50}s were also determined with 1 μM CaCYP51 (C) and 0.4 μM Δ60HsCYP51 (D) for the agricultural azoles epoxiconazole (●), prochloraz (■), propiconazole (▲), tebuconazole (◆), triadimenol (○), prothioconazole (□), and prothioconazole-desthio (△) with itraconazole (⊙) as a control. Relative velocities of 1.00 correspond to actual velocities of 3.9 ± 0.3 min^{-1} for CaCYP51 and 22.7 ± 4.8 min^{-1} for Δ60HsCYP51.

TABLE 3 IC_{50}s for azole antifungal agents with CaCYP51 and Δ60HsCYP51

Azole antifungal agent	IC_{50} (μM)	
	CaCYP51	Δ60HsCYP51
Medical azoles		
Fluconazole	0.6	~1,300[a]
Itraconazole	0.4	70
Ketoconazole	0.5	4.5
Agricultural azoles		
Epoxiconazole	0.5	12
Prochloraz	0.7	8
Propiconazole	0.6	110
Prothioconazole	150	None[b]
Prothioconazole-desthio	0.6	100
Tebuconazole	0.9	1.3
Triadimenol	1.3	30

[a] Only 25% inhibition of Δ60HsCYP51 activity occurred in the presence of 653 μM fluconazole. The estimated IC_{50} for fluconazole is greater than 1,300 μM.
[b] No significant inhibition of Δ60HsCYP51 activity occurred in the presence of 290 μM prothioconazole.

zole. Prothioconazole was the exception, as it did not significantly inhibit CaCYP51 activity at concentrations up to 4 μM. The prothioconazole concentration had to be increased to 145 μM for us to observe a 48% reduction in the CaCYP51 activity.

In general, inhibition of 0.4 μM Δ60HsCYP51 by the agricultural azoles (Fig. 7D) was less severe than that of 1 μM CaCYP51, although it was still significant. Tebuconazole, prochloraz, epoxiconazole, and triadimenol proved more effective at inhibiting Δ60HsCYP51 than itraconazole, with IC_{50}s of 1.3, 8, 12, and 30 μM, respectively, compared to 70 μM for itraconazole. The severe inhibition caused by tebuconazole approached that seen with itraconazole and CaCYP51. Both prothioconazole-desthio and propiconazole inhibited Δ60HsCYP51 with potencies similar to that of itraconazole, with IC_{50}s of 100 and 110 μM, respectively. The residual Δ60HsCYP51 activity levels at the highest azole concentration tested increased progressively from 9% for tebuconazole to 10% for prochloraz, 16% for epoxiconazole, 18% for triadimenol, 34% for propiconazole, and 35% for prothioconazole-desthio, in comparison with 32% for itraconazole, indicating that lanosterol was able to displace these azoles from Δ60HsCYP51 in the CYP51 reconstitution assay. In contrast, prothioconazole did not cause any significant inhibition of Δ60HsCYP51 activity at concentrations up to 290 μM.

DISCUSSION

Previous studies with HsCYP51 (16, 18, 46) established that clotrimazole, ketoconazole, and itraconazole bound tightly to HsCYP51 (K_ds, 0.10 to 0.13 μM, 0.11 to 0.19 μM, and 3.6 μM, respectively), while fluconazole bound weakly to HsCYP51 (K_ds, 40 to 200 μM). This was in broad agreement with our findings except those for itraconazole, which bound 30- to 40-fold more tightly in our study. This reaffirms the therapeutic selectivity of fluconazole (540-fold) and voriconazole (220-fold) for *C. albicans* CYP51 target enzymes over the host human CYP51 and the efficacy of intravenous administration of fluconazole in the treatment of systemic *Candida* infections, with minimal side effects on the patient's native CYP51. Clotrimazole, ketoconazole, and itraconazole, however, have shown less selectivity toward CaCYP51 (K_ds, 10 to 26 nM) over the host human CYP51 (K_ds, 42 to 131 nM), and itraconazole is the main drug used for systemic rather than superficial infections. IC_{50} studies with the medical azoles fluconazole, itraconazole, and ketoconazole confirmed that all three azoles severely inhibited CaCYP51 and that ketoconazole strongly inhibited Δ60HsCYP51, whereas fluconazole only weakly inhibited Δ60HsCYP51. Interestingly, itraconazole only moderately inhibited Δ60HsCYP51, with 32% residual CYP51 activity observed in the presence of 283 μM itraconazole, indicating that lanosterol readily displaces itraconazole from the heme environment of Δ60HsCYP51. Therefore, the azole binding constants (K_ds) cannot be used on their own to accurately predict the inhibitory potency of azole antifungal agents with Δ60HsCYP51. The itraconazole affinities of the truncated Δ60HsCYP51 and full-length HsCYP51 were similar (K_ds, 92 and 131 nM, respectively), suggesting that similar IC_{50}s for itraconazole would be obtained and that the weak itraconazole inhibition observed was an innate property of HsCYP51, in contrast to CaCYP51.

Previously, Trösken et al. (47) compared the effectiveness of medical and agricultural azole antifungal agents on CaCYP51 and HsCYP51 by performing IC_{50} determinations using CYP51 reconstitution assays containing 0.2 μM CaCYP51 or 0.1 μM HsCYP51 expressed in insect microsomes. Trösken et al. (47) demonstrated that the medical azoles clotrimazole, fluconazole, itraconazole, and ketoconazole bound tightly to CaCYP51 (IC_{50}s, 0.2 to 0.45 times the CaCYP51 concentration), with HsCYP51 IC_{50}s for ketoconazole, fluconazole, and itraconazole that were 4.3-, >300-, and ~300-fold greater than the HsCYP51 concentration. This was in agreement with our findings except that we found itraconazole to be a more potent inhibitor of HsCYP51 activity.

The agricultural azoles, with the exception of prothioconazole, bound tightly to both CaCYP51 and Δ60HsCYP51, with little selectivity for the *C. albicans* enzyme over the human homolog (only 3- to 9-fold). Tight binding of the agricultural azoles epoxiconazole, tebuconazole, and triadimenol was also previously observed with *Mycosphaerella graminicola* CYP51 (48), yielding K_d values of 16.6, 26.6, and 299 nM, respectively, indicating that triadimenol was 4-fold more selective for CaCYP51 than *M. graminicola* CYP51. Strushkevich et al. (46) previously determined K_d values for propiconazole, tebuconazole, and triadimenol of 0.17, <0.10, and 0.19 μM, respectively, with HsCYP51, which were in agreement with our findings. Interestingly, the main mammalian metabolite of prothioconazole, i.e., prothioconazole-desthio (49, 50), bound tightly to both CaCYP51 and Δ60HsCYP51, with equal affinities (K_d, ~40 nM), whereas the parent compound only weakly associated with both CYP51 enzymes, as previously observed with *M. graminicola* CYP51 (48).

IC_{50} studies with the agricultural azoles epoxiconazole, prochloraz, propiconazole, prothioconazole, prothioconazole-desthio, tebuconazole, and triadimenol confirmed that all of them except prothioconazole severely inhibited CaCYP51 activity (IC_{50}s, 0.5 to 1.3 μM), and these IC_{50}s are largely in agreement with the K_d values (Table 2). However, the agricultural azole IC_{50}s with Δ60HsCYP51 were more variable. Tebuconazole, prochloraz, and epoxiconazole strongly inhibited Δ60HsCYP51 activity (IC_{50}s, 1.3, 8, and 12 μM, respectively), with tebuconazole approaching the potency of itraconazole with CaCYP51. Propiconazole and prothioconazole-desthio inhibited Δ60HsCYP51 moderately and with the same severity as itraconazole (IC_{50}s, 110, 100, and 70 μM, respectively). Triadimenol inhibited Δ60HsCYP51 activity with an effect between those of tebucona-

zole and itraconazole (IC_{50}, 30 μM). Interestingly, the 60 μM lanosterol in the CYP51 assay displaced all of the agricultural azoles and itraconazole from Δ60HsCYP51 to varying degrees, with residual CYP51 activities at the highest azole concentration used (280 to 330 μM) of 9% for tebuconazole, 10% for prochloraz, 16% for epoxiconazole, 18% for triadimenol, 34% for propiconazole, 35% for prothioconazole, and 32% for itraconazole, explaining why the inhibition observed was not as severe as predicted by the azole K_d values (Table 2). We previously showed that epoxiconazole noncompetitively inhibits the binding of eburicol to *M. graminicola* CYP51 (48), as azole antifungal agents bind to the CYP51 molecule primarily through direct coordination with the heme prosthetic group and not through interactions with the substrate binding site (36). To establish whether increasing lanosterol concentrations relieve azole antifungal inhibition of CaCYP51 and Δ60HsCYP51 activities by a competitive or noncompetitive kinetic mechanism, IC_{50} experiments need to be performed with several different lanosterol concentrations. However, the physiological relevance of using higher lanosterol concentrations is questionable. Trösken et al. (47) established that the agricultural azoles epoxiconazole, prochloraz, propiconazole, tebuconazole, and triadimenol bound tightly to CaCYP51 (IC_{50}s, 0.5 to 1.75 times the CaCYP51 concentration), whereas binding of these agricultural azoles to HsCYP51 was much weaker (IC_{50}s, 19- to 370-fold greater than the HsCYP51 concentration), in keeping with our IC_{50} findings for Δ60HsCYP51, which were 3-fold (tebuconazole) to 3,250-fold (fluconazole) higher than the HsCYP51 concentration.

Prothioconazole was alone in only weakly inhibiting CaCYP51 (IC_{50}, ~150 μM) and failing to inhibit Δ60HsCYP51 even at 290 μM, probably due to the sulfur atom covalently linked to the triazole ring sterically impeding the N-4 nitrogen atom from coordinating directly with the CYP51 heme ferric ion as the sixth axial ligand. This suggests that the active form of prothioconazole, one of the major agricultural azoles currently in use, is the desthio form generated by intracellular metabolism in mammals (49, 50) and in other organisms or by physicochemical means (such as temperature and/or photoactivation) on the surface of plants. With the sulfur atom removed from the triazole ring, the N-4 nitrogen atom can efficiently coordinate with the CYP51 heme ferric ion, inhibiting CYP51 activity.

The relatively poor selectivity of the agricultural azoles for the fungal CYP51 over the human homolog raises the concern that exposure to azole fungicide residues might disrupt sterol biosynthesis and other endogenous downstream cytochrome P450 metabolic systems, such as human steroidogenesis and phase I metabolism of xenobiotics in the liver. Ayub and Levell (51–54) found that human CYP19 was inhibited strongly by econazole, tioconazole, bifoconazole, miconazole, isoconazole, and clotrimazole (IC_{50}, 0.25 to 0.67 μM), whereas ketoconazole was less potent (IC_{50}, 7.3 μM), and CYP17 was inhibited by azole antifungals (IC_{50}, 0.6 to 4 μM). In comparison, prochloraz, propiconazole, and triadimenol inhibited CYP19, with IC_{50}s of 0.04, 6.5, and 21 μM, respectively (55), indicating that agricultural azoles have the general ability to inhibit the P450 enzymes in steroidogenesis, albeit with different potencies. Since the introduction of large-scale use of azole antifungals in the late 1980s, increasing evidence of hepatotoxicity and associated hepatic tumors has been reported (56, 57), with liver tissue concentrations of ketoconazole and itraconazole being reported as 22- and 10-fold higher, respectively, than plasma levels (58), indicating azole toxicity in the liver being more acute than in other tissues. This reaffirms the need for further research to establish the interactions of the agricultural azoles and their metabolites with the human cytochrome P450 complement. In addition, recent evidence indicates that the L98H point mutation in *Aspergillus fumigatus* CYP51A, which confers resistance to medical azole antifungals, was acquired through exposure to agricultural azoles outside the clinic, in the general environment (6–8), which highlights the need to adopt a more comprehensive approach to azole antifungal design and treatment regimens both in the clinic and in agriculture to improve azole antifungal specificity, including that against HsCYP51.

ACKNOWLEDGMENT

We are grateful to the Engineering and Physical Sciences Research Council National Mass Spectrometry Service Centre at Swansea University for assistance.

REFERENCES

1. **Kelly SL, Lamb DC, Jackson CJ, Warrilow AGS, Kelly DE.** 2003. The biodiversity of microbial cytochromes P450. Adv. Microb. Physiol. **47**:131–186.
2. **Lamb DC, Kelly DE, Waterman MR, Stromstedt M, Rozman D, Kelly SL.** 1999. Characteristics of the heterologously expressed human lanosterol 14α-demethylase (other names: P45014DM, CYP51, P45051) and inhibition of the purified human and *Candida albicans* CYP51 with azole antifungal agents. Yeast **15**:755–763.
3. **Parker JE, Merkamm M, Manning NJ, Pompon D, Kelly SL, Kelly DE.** 2008. Differential azole antifungal efficacies contrasted using a *Saccharomyces cerevisiae* strain humanized for sterol 14α-demethylase at the homologous locus. Antimicrob. Agents Chemother. **52**:3597–3603.
4. **Warrilow AGS, Martel CM, Parker JE, Melo N, Lamb DC, Nes D, Kelly DE, Kelly SL.** 2010. Azole binding properties of *Candida albicans* sterol 14-α demethylase (CaCYP51). Antimicrob. Agents Chemother. **54**:4235–4245.
5. **Jefcoate CR, Gaylor JL, Calabrese RL.** 1969. Ligand interactions with cytochrome P450. I. Binding of primary amines. Biochemistry **8**:3455–3463.
6. **Verweij PE, Snelders E, Kema GHJ, Mellado E, Melchers WJ.** 2009. Azole resistance in *Aspergillus fumigatus*: a side-effect of environmental fungicide use? Lancet Infect. Dis. **9**:789–795.
7. **Snelders E, Huis in't Veld RAG, Rijs AJMM, Kema GHJ, Melchers WJG, Verweij PE.** 2009. Possible environmental origin of resistance of *Aspergillus fumigatus* to medical triazoles. Appl. Environ. Microbiol. **75**:4053–4057.
8. **Snelders E, Camps SMT, Karawajczyk A, Schaftenaar G, Kema GH, van der Lee HA, Klaassen CH, Melchers WJG, Verweij PE.** 2012. Triazole fungicides can induce cross-resistance to medical triazoles in *Aspergillus fumigatus*. PLoS One **7**:e31801. doi:10.1371/journal.pone.0031801.
9. **Cools HJ, Mullins JGL, Fraaije BA, Parker JE, Kelly DE, Lucas JA, Kelly SL.** 2011. Impact of recently emerged sterol 14α-demethylase (CYP51) variants of *Mycosphaerella graminicola* on azole fungicide sensitivity. Appl. Environ. Microbiol. **77**:3830–3837.
10. **Howard SJ, Cerar D, Anderson MJ, Albarrag A, Fisher MC, Pasqualotto AC, Laverdiere M, Arendrup MC, Perlin DS, Denning DW.** 2009. Frequency and evolution of azole resistance in *Aspergillus fumigatus* associated with treatment failure. Emerg. Infect. Dis. **15**:1068–1076.
11. **Pfaller MA, Diekema DJ.** 2007. Epidemiology of invasive candidiasis: a persistent public health problem. Clin. Microbiol. Rev. **20**:133–163.
12. **Richardson MD.** 2007. Changing patterns and trends in systemic fungal infections. J. Antimicrob. Chemother. **56**(Suppl 1):i5–i11.
13. **Sims CR, Ostrosky-Zeichner L, Rex JH.** 2005. Invasive candidiasis in immunocompromised hospitalized patients. Arch. Med. Res. **36**:660–671.
14. **Snelders E, van der Lee HAL, Kuijpers J, Rijs AJMM, Varga J, Samson RA, Mellado E, Donders AR, Melchers WJG, Verweij PE.** 2008. Emergence of azole resistance in *Aspergillus fumigatus* and spread of a single resistance mechanism. PLoS Med. **5**:e219. doi:10.1371/journal.pmed.0050219.
15. **Doyle PS, Chen CK, Johnston JB, Hopkins SD, Leung SSF, Jacobson MP, Engel JC, McKerrow JH, Podust LM.** 2010. A nonazole CYP51 inhibitor cures Chagas' disease in a mouse model of acute infection. Antimicrob. Agents Chemother. **54**:2480–2488.

16. **Ekins S, Mankowski DC, Hoover DJ, Lawton MP, Treadway JL, Harwood HJ.** 2007. Three-dimensional quantitative structure-activity relationship analysis of human CYP51 inhibitors. Drug Metab. Dispos. **35**: 493–500.
17. **Konkle ME, Hargrove TY, Kleshchenko YY, von Kries JO, Ridenour W, Uddin J, Caprioli RM, Marnett LJ, Nes WD, Villalta F, Waterman MR, Lepesheva GI.** 2009. Indomethacin amides as a novel molecular scaffold for targeting *Trypanosoma cruzi* sterol 14α-demethylase. J. Med. Chem. **52**:2846–2853.
18. **Korosec T, Acimovic J, Seliskar M, Kocjan D, Tacer KF, Rozman D, Urleb U.** 2008. Novel cholesterol biosynthesis inhibitors targeting human lanosterol 14α-demethylase (CYP51). Bioorg. Med. Chem. **16**:209–221.
19. **Lepesheva GI, Ott RD, Hargrove TY, Kleshchenko YY, Schuster I, Nes WD, Hill GC, Villalta F, Waterman MR.** 2007. Sterol 14α-demethylase as a potential target for antitrypanosomal therapy: enzyme inhibition and parasite cell growth. Chem. Biol. **14**:1283–1293.
20. **Podust LM, von Kries JP, Eddine AN, Kim Y, Yermalitskaya LV, Kuehne R, Ouellet H, Warrier T, Alteköster M, Lee JS, Rademann J, Oschkinat H, Kaufmann SHE, Waterman MR.** 2007. Small-molecule scaffolds for CYP51 inhibitors identified by high-throughput screening and defined by X-ray crystallography. Antimicrob. Agents Chemother. **51**:3915–3923.
21. **Podust LM, Ouellet H, von Kries JP, Ortiz de Montellano P.** 2009. Interaction of *Mycobacterium tuberculosis* CYP130 with heterocyclic arylamines. J. Biol. Chem. **284**:25211–25219.
22. **Zhang J, Zhao L, Zhang J, Han R, Li S, Yuan Y, Xiao W, Liu D.** 2010. Optimised expression and spectral analysis of the target enzyme CYP51 from *Penicillium digitatum* with possible new DMI fungicides. Pest. Manag. Sci. **66**:1344–1350.
23. **Taxvig C, Vinggaard M, Hass U, Axelstad M, Metzdorff S, Nellemann C.** 2008. Endocrine-disrupting properties *in vivo* of widely used azole fungicides. Int. J. Androl. **31**:170–177.
24. **Sanderson JT.** 2006. The steroid hormone biosynthesis pathway as a target for endocrine-disrupting chemicals. Toxicol. Sci. **94**:3–21.
25. **Korashy HM, Shayeganpour A, Brocks DR, El-Kadi AOS.** 2007. Induction of cytochrome P450 1A1 by ketoconazole and itraconazole but not fluconazole in murine and human hepatoma cell lines. Toxicol. Sci. **97**:32–43.
26. **Nesnow S, Padgett WT, Moore T.** 2011. Propiconazole induces alterations in the hepatic metabolome of mice: relevance to propiconazole-induced hepatocarcinogenesis. Toxicol. Sci. **120**:297–309.
27. **Babin M, Casado S, Chana A, Herradon B, Segner H, Tarazona JV, Navas JM.** 2005. Cytochrome P4501A induction caused by the imidazole prochloraz in rainbow trout cell line. Toxicol. In Vitro **19**:899–902.
28. **Hasselberg L, Grosvik BE, Goksoyr A, Celander MC.** 2005. Interactions between xenoestrogens and ketoconazole on hepatic CYP1A and CYP3A in juvenile Atlantic cod (*Gadus morhua*). Comp. Hepatol. **4**:2. doi:10.1186/1476-5926-4-2.
29. **Pont A, Williams PL, Azhar S, Reitz RE, Bochra C, Smith ER, Stevens DA.** 1982. Ketoconazole blocks testosterone synthesis. Arch. Intern. Med. **142**:2137–2140.
30. **Pont A, Williams PL, Loose DS, Feldman D, Reitz RE, Bochra C, Stevens DA.** 1982. Ketoconazole blocks adrenal steroid synthesis. Ann. Intern. Med. **97**:370–372.
31. **Thompson DF, Carter JR.** 1993. Drug-induced gynecomastia. Pharmacotherapy **13**:37–45.
32. **Lepesheva GI, Park HW, Hargrove TY, Vanhollebeke B, Wawrzak Z, Harp JM, Sundaramoorthy M, Nes WD, Pays E, Chaudhuri M, Villalta F, Waterman MR.** 2010. Crystal structures of *Trypanosoma brucei* sterol 14α-demethylase and implications for selective treatment of human infections. J. Biol. Chem. **285**:1773–1780.
33. **von Wachenfeldt C, Richardson TH, Cosme J, Johnson EF.** 1997. Microsomal P450 2C3 is expressed as a soluble dimer in *Escherichia coli* following modifications of its N-terminus. Arch. Biochem. Biophys. **339**:107–114.
34. **Barnes HJ, Arlotto MP, Waterman MR.** 1991. Expression and enzymatic activity of recombinant cytochrome P450 17α-hydroxylase in *Escherichia coli*. Proc. Natl. Acad. Sci. U. S. A. **88**:5597–5601.
35. **Arase M, Waterman MR, Kagawa N.** 2006. Purification and characterization of bovine steroid 21-hydroxylase (P450c21) efficiently expressed in *Escherichia coli*. Biochem. Biophys. Res. Commun. **344**:400–405.
36. **Bellamine A, Mangla AT, Nes WD, Waterman MR.** 1999. Characterization and catalytic properties of the sterol 14α-demethylase from *Mycobacterium tuberculosis*. Proc. Natl. Acad. Sci. U. S. A. **96**:8937–8942.
37. **Estabrook RW, Peterson JA, Baron J, Hildebrandt AG.** 1972. The spectrophotometric measurement of turbid suspensions of cytochromes associated with drug metabolism, p 303–350. *In* Chignell CF (ed), Methods in pharmacology, vol 2. Appleton-Century-Crofts, New York, NY.
38. **Omura T, Sato R.** 1964. The carbon monoxide-binding pigment of liver microsomes. J. Biol. Chem. **239**:2379–2385.
39. **Venkateswarlu K, Denning DW, Manning NJ, Kelly SL.** 1995. Resistance to fluconazole in *Candida albicans* from AIDS patients correlated with reduced intracellular accumulation of drug. FEMS Microbiol. Lett. **131**: 337–341.
40. **Lutz JD, Dixit V, Yeung CK, Dickmann LJ, Zelter A, Thatcher JA, Nelson WL, Isoherranen N.** 2009. Expression and functional characterization of cytochrome P450 26A1, a retinoic acid hydroxylase. Biochem. Pharmacol. **77**:258–268.
41. **Morrison JF.** 1969. Kinetics of the reversible inhibition of enzyme-catalysed reactions by tight-binding inhibitors. Biochim. Biophys. Acta **185**:269–286.
42. **Copeland RA.** 2005. Evaluation of enzyme inhibitors in drug discovery: a guide for medicinal chemists and pharmacologists, p 178–213. Wiley-Interscience, New York, NY.
43. **Bellamine A, Lepesheva GI, Waterman MR.** 2004. Fluconazole binding and sterol demethylation in three CYP51 isoforms indicate differences in active site topology. J. Lipid Res. **45**:2000–2007.
44. **Lepesheva GI, Podust LM, Bellamine A, Waterman MR.** 2001. Folding requirements are different between sterol 14α-demethylase (CYP51) from *Mycobacterium tuberculosis* and human or fungal orthologs. J. Biol. Chem. **276**:28413–28420.
45. **Jefcoate CR.** 1978. Measurement of substrate and inhibitor binding to microsomal cytochrome P-450 by optical-difference spectroscopy. Methods Enzymol. **52**:258–279.
46. **Strushkevich N, Usanov SA, Park H-W.** 2010. Structural basis of human CYP51 inhibition by antifungal azoles. J. Mol. Biol. **397**:1067–1078.
47. **Trösken ER, Adamska M, Arand M, Zarn JA, Patten C, Völkel W, Lutz WK.** 2006. Comparison of lanosterol-14α-demethylase (CYP51) of human and *Candida albicans* for inhibition by different antifungal azoles. Toxicology **228**:24–32.
48. **Parker JE, Warrilow AGS, Cools HJ, Martel CM, Nes WD, Fraaije BA, Lucas JA, Kelly DE, Kelly SL.** 2011. Mechanism of binding of prothioconazole to *Mycosphaerella graminicola* CYP51 differs from that of other azole antifungals. Appl. Environ. Microbiol. **77**:1460–1465.
49. **Australian Pesticides and Veterinary Medicines Authority.** 2007. Evaluation of the new active prothioconazole in the product Redigo fungicidal seed treatment. Australian Pesticides and Veterinary Medicines Authority, Canberra, Australia.
50. **Food and Agriculture Organization of the United Nations, World Health Organization.** 2008. Pesticide residues in food 2008: joint FAO/WHO meeting on pesticide residues. FAO plant production and protection paper 193, p 265–292. World Health Organization, New York, NY.
51. **Ayub M, Levell MJ.** 1987. Inhibition of testicular 17α-hydroxylase and 17,20-lyase but not 3β-hydroxysteroid dehydrogenase-isomerase or 17β-hydroxysteroid oxidoreductase by ketoconazole and other imidazole drugs. J. Steroid Biochem. **28**:521–531.
52. **Ayub M, Levell MJ.** 1988. Structure-activity relationships of the inhibition of human placental aromatase by imidazole drugs including ketoconazole. J. Steroid Biochem. **31**:65–72.
53. **Ayub M, Levell MJ.** 1989. Inhibition of human adrenal steroidogenic enzymes *in vitro* by imidazole drugs including ketoconazole. J. Steroid Biochem. **32**:515–524.
54. **Ayub M, Levell MJ.** 1990. The inhibition of human prostatic aromatase activity by imidazole drugs including ketoconazole and 4-hydroxyandrostenedione. Biochem. Pharmacol. **40**:1569–1575.
55. **Vinggaard AM, Hnida M, Breinholt V, Larsen JC.** 2000. Screening of selected pesticides for inhibition of CYP19 aromatase activity *in vitro*. Toxicol. In Vitro **14**:227–234.
56. **Juberg DR, Mudra DR, Hazelton GA, Parkinson A.** 2006. The effect of fenbuconazole on cell proliferation and enzyme induction in the liver of female CD1 mice. Toxicol. Appl. Pharmacol. **214**:178–187.
57. **Sun G, Thai S, Tully DB, Lambert GR, Goetz AK, Wolf DC, Dix DJ, Nesnow S.** 2005. Propiconazole-induced cytochrome P450 gene expression and enzymatic activities in rat and mouse liver. Toxicol. Lett. **155**:277–287.
58. **Prentice AG, Glasmacher A.** 2005. Making sense of itraconazole pharmacokinetics. J. Antimicrob. Chemother. **56**(Suppl 1):i17–i22.